

## DOMAIN OF RESEARCH :

# PINNING OF VORTICES IN SINGLE CRYSTALS HIGH- $T_c$ OXIDE SUPERCONDUCTORS

**Dr. Prof. Samir Khène**

Department of Physics, Faculty of Sciences, Badji Mokhtar University,

BP 12, 23000 Annaba, Algeria

Tel/Fax: +213-38-87-53-99

Email: samirkhene@yahoo.fr

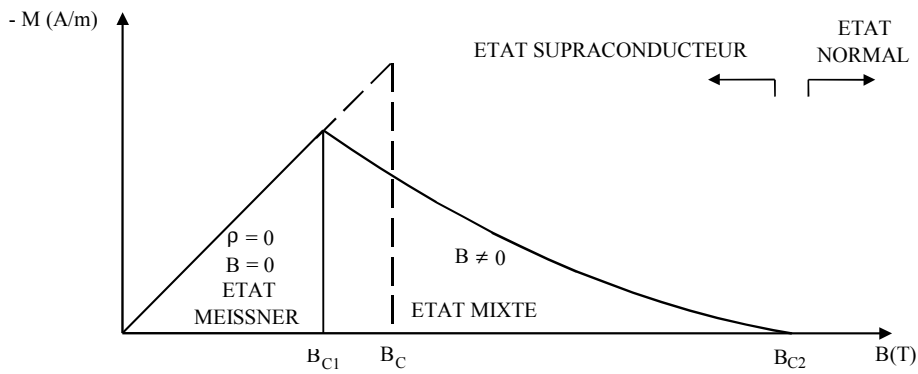
☞ Studies on the superconducting properties have two objectives :

① From the basic point of view the important problem is to clarify the mechanism of the high- $T_c$  superconductivity and to discover materials with higher  $T_c$ .

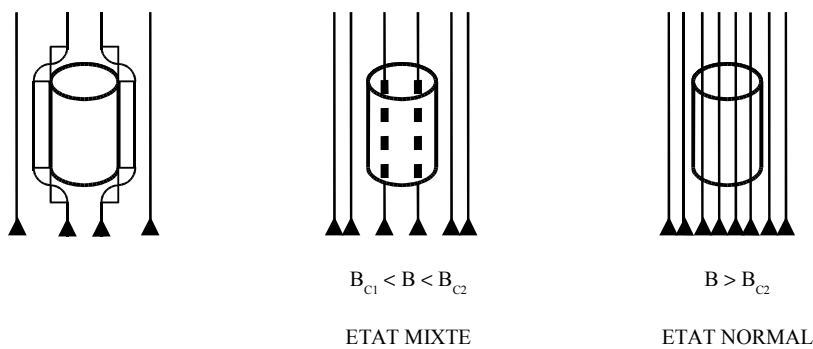
② From a practical point of view the problem is to find the mechanism of strong pinning of vortices and to obtain samples with higher critical current density. These later can be used for making wires for the production of magnetic fields.

☞ There are two kinds of pinning :

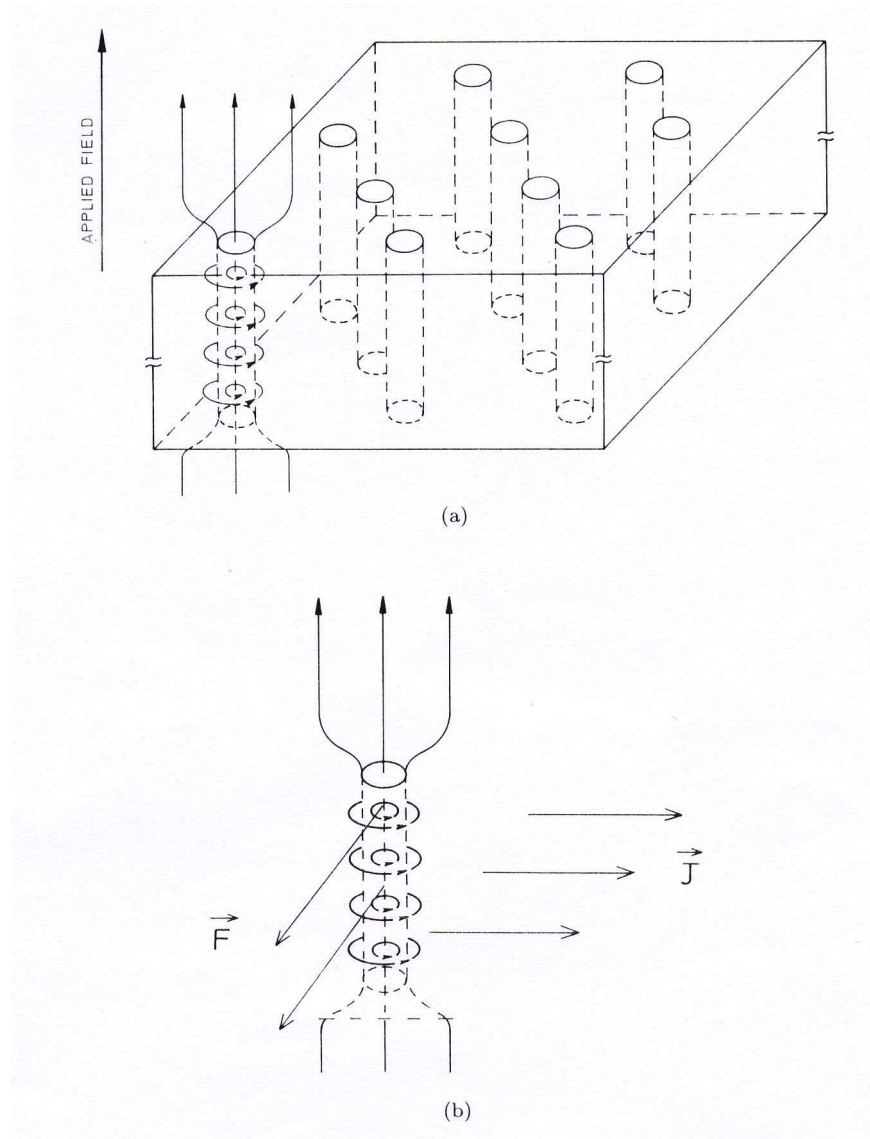
- Intrinsic
- Extrinsic



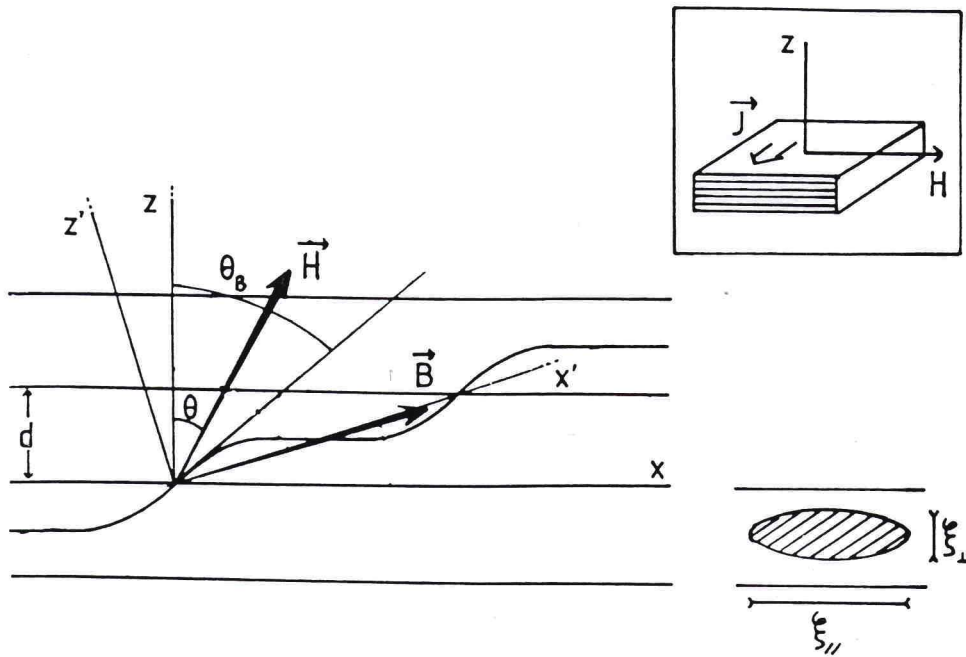
Magnetization as a function of the magnetic field for a type II superconductor. In the mixed state, the Meissner effect is partial.



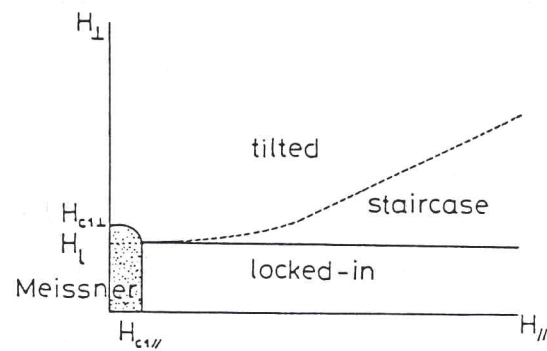
Different states in a type II superconductor (adapted from M. Decroux et Q. Fisher).



(a) Schematic representation of the mixed state where the vortices form a hexagonal lattice. (b) The Lorentz force  $\mathbf{f}$  which acts on a flux line in the presence of the current  $\mathbf{J}$  (adapted from Buckel, after M. Cyrot et D. Pavuna).



Flux line shape for an oblique field. The direction of the field  $H$  and the local line direction are respectively defined by  $\theta$  and  $\theta_B$ . Inset shows the configuration for a parallel field and an intrinsic pinning (after D. Feinberg and C. Villard).



Phase diagram showing the lock-in transition line in the quasi-2D regime ( $\lambda_J < \lambda_{\parallel}$ ). The dotted line corresponds to  $\tan\varphi = \gamma$ , i.e., the appearance of staircase vortices (after D. Feinberg and A. M. Ettouhami).

## VORTICES PINNING INTRINSIC

In the high- $T_C$  oxide superconductors, the coherence length along the  $c$  axis is very short. Consequently, the layer structure itself works as strong pinning centers of vortices. The critical current density estimated from pinning mechanism is very high comparable to the critical current density measured in thin films of high quality.

**AIM OF THIS STUDY :** Using a double squid magnetometer and a  $\text{La}_{1.85}\text{Sr}_{0.15}\text{CuO}_4$  single crystal, we confirm, in the reversible domain and by different ways, the existence of the lock-in transition of vortices by rotational magnetization measurements in the quasi-2D regime.

**Keywords :** high- $T_C$  superconductors, Lock-in transition,  $\text{La}_{1.85}\text{Sr}_{0.15}\text{CuO}_4$ , Pinning effects, Magnetic anisotropy, Mixed state, Flux lines configuration.

• **Acknowledgements :**

I would like to thank D. Feinberg for fruitful discussions and S. Senoussi for having lent us the LSCO single crystal. I would also like to thank warmly G. Fillion and B. Barbara of Louis Néel Laboratory (Grenoble) for their hospitality and for the use of large scientific facilities.

## MAIN PREDICTIONS OF THE LOCK-IN TRANSITION THEORY

(D. Feinberg and A. M. Ettouhami, *International Journal of Modern Physics B*, Vol.7, N°11 (1993) 2085)

- A layered structure and a very short coherence length along the direction perpendicular to CuO<sub>2</sub> planes characterize the high T<sub>C</sub> superconductors. This has given birth to novel properties that are important for the applications to come. The lock-in transition is the one of these properties.
- For fields applied closer to CuO<sub>2</sub> planes than some critical angle both field and temperature dependent, the increase in energy required for flux lines crossing the planes makes the configuration parallel to the planes more favourable than any other.
- The lock-in transition is an equilibrium property of the flux line lattice which must be identified in reversible conditions.
- When the direction of vortices rocks to become parallel to CuO<sub>2</sub> planes, the angle between the vortices and the applied field increases suddenly.
- In the locked state, all the vortices sit between the CuO<sub>2</sub> planes and parallel to these later.
- The appearance of two maximums in the angular variation of the transverse magnetization. The London-Kogan maximum first occurs followed by the lock-in transition maximum.
- The shifting of the angular positions of the lock-in transverse magnetization maximums towards the lower angles when the applied field decreases.
- Close to 90°, the M<sub>Xrev</sub> slope must be proportional to the applied field H.

$$\left. \frac{dM_{Xrev}}{d\theta} \right|_{90^\circ} = \frac{H}{4\pi(1 - N_{\perp})} \quad (1)$$

- In the quasi-2D regime, the normal component of the internal field is of the order of lower critical field normal to planes but smaller in the quasi-3D regime.

$$H \frac{\cos\theta_L}{1 - N_{\perp}} = H_{\perp} \approx H_{c1\perp} \quad (2)$$

# EXPERIMENTAL PROCEDURE

## ☞ Physical features of the used sample :

- a  $\text{La}_{1.85}\text{Sr}_{0.15}\text{CuO}_4$  single crystal
- $T_C = 35 \text{ K}$
- dimensions :  $1.85 \times 1.30 \times 0.8 \text{ mm}^3$
- mass  $\approx 11 \text{ mg}$
- grown by travelling solvent floating method
- prepared by I. Tanaka and H. Kojima (Japan)

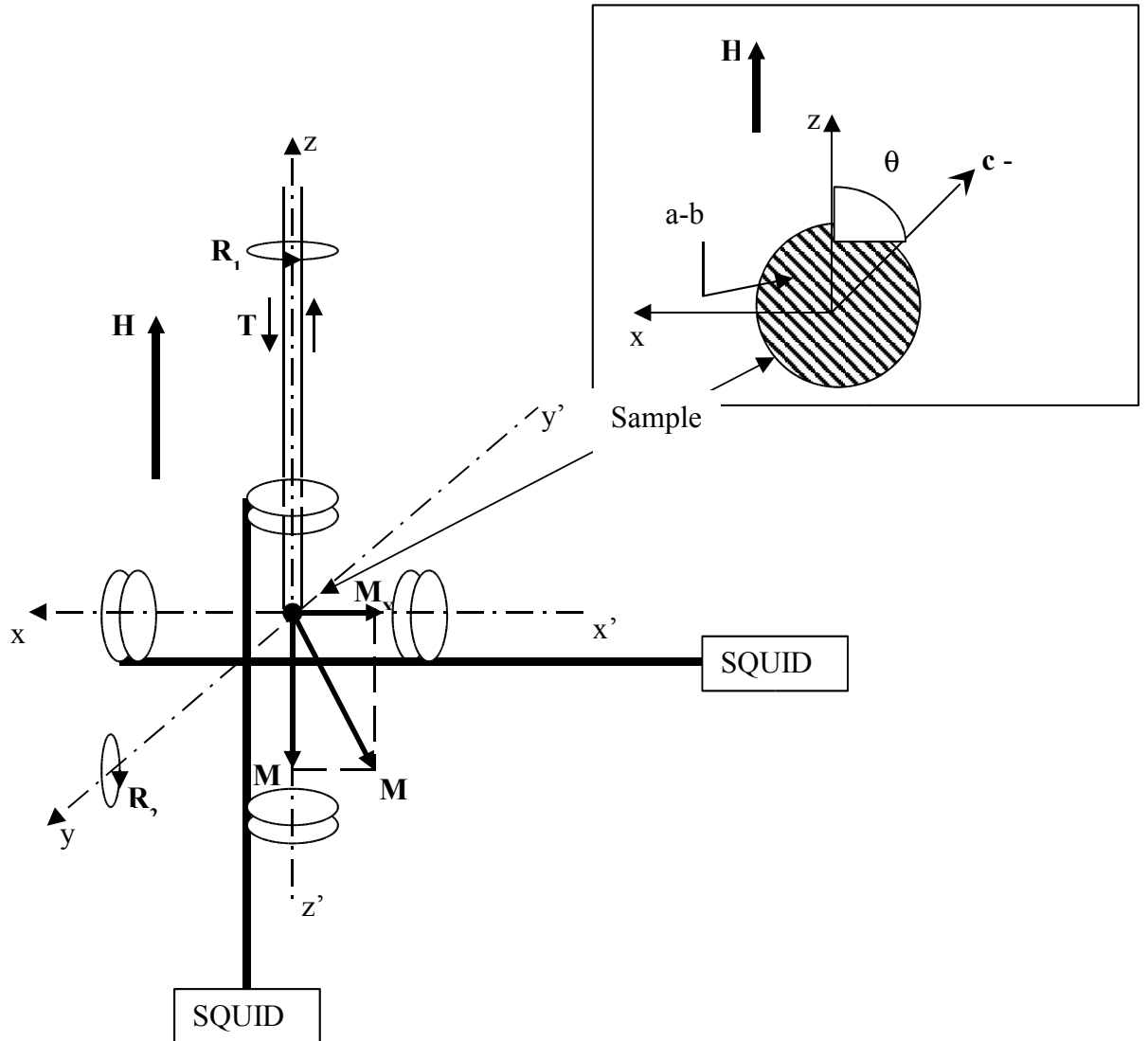
## ☞ Characteristics of the used magnetometer :

- a pick- double squid magnetometer endowed with a pair of orthogonal up coils
- able to measure simultaneously the transverse ( $M_X$ ) and longitudinal ( $M_Z$ ) components of the magnetization
- It enables the rotation both ways of the sample relative to the applied field  $H$
- a sensitivity of the order of  $10^{-7} \text{ emu}$

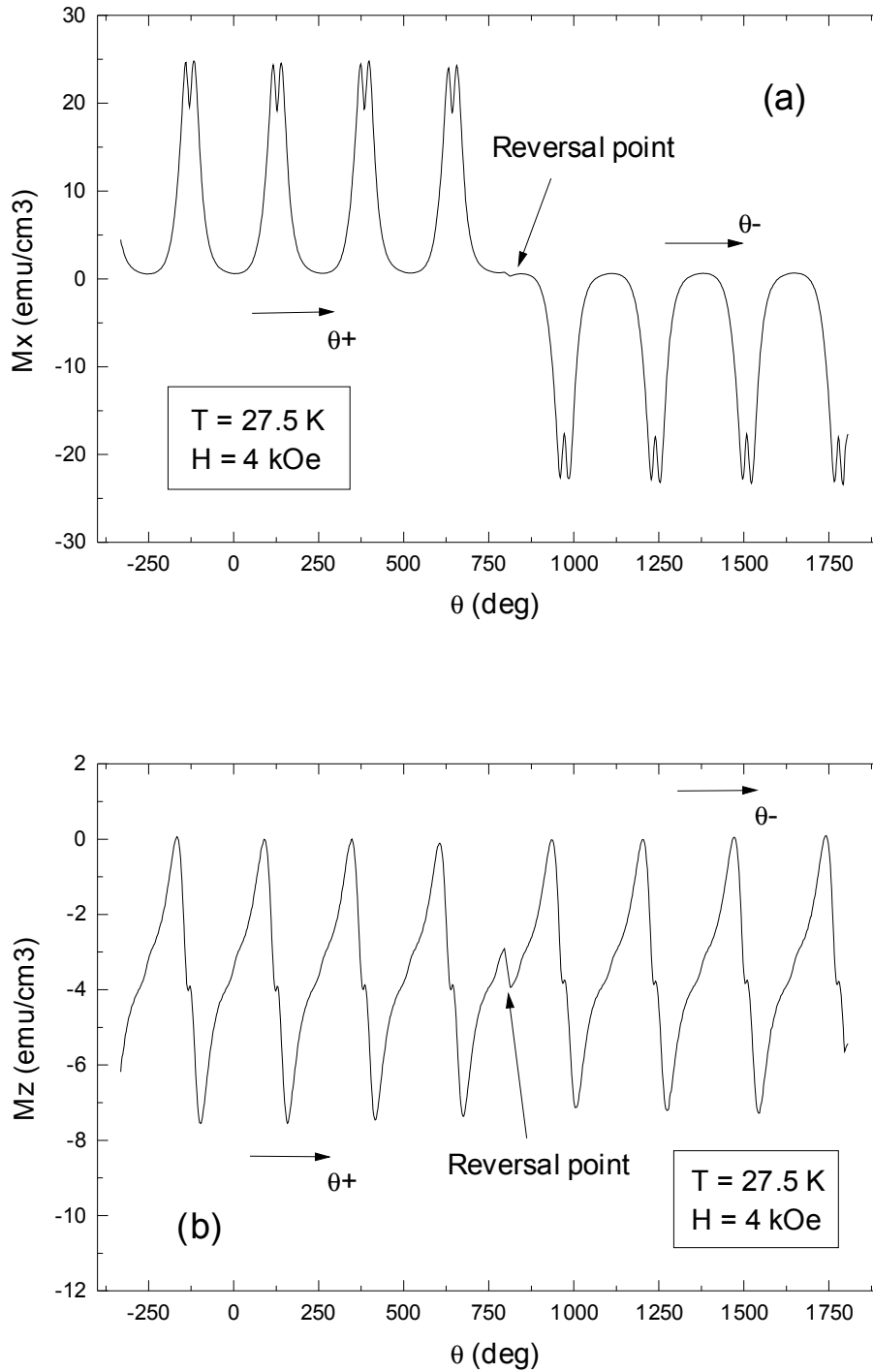
## ☞ measuring magnetization components steps :

- ① the sample temperature has been increased to a temperature greater than the critical temperature  $T_C$ , then it has been decreased to the selected one (the temperature stability is always better than  $\pm 0.03 \text{ K}$ ), in the absence of external field (Zero Field Cooled Method).
- ② the sample has been submitted to a magnetic field stronger than  $H_{C1}$ .
- ③ while rotating the sample in both senses with continuous velocity of  $0.3^\circ/\text{s}$ , the magnetization components have been measured under constant field and temperature.
- ④ the previous steps have been reapplied for three temperatures in the neighbourhood of  $T_C$  (27.5 K, 29.5 K and 31.5 K). For each temperature, the magnetic field has been gradually increased within 2 – 10 kOe.

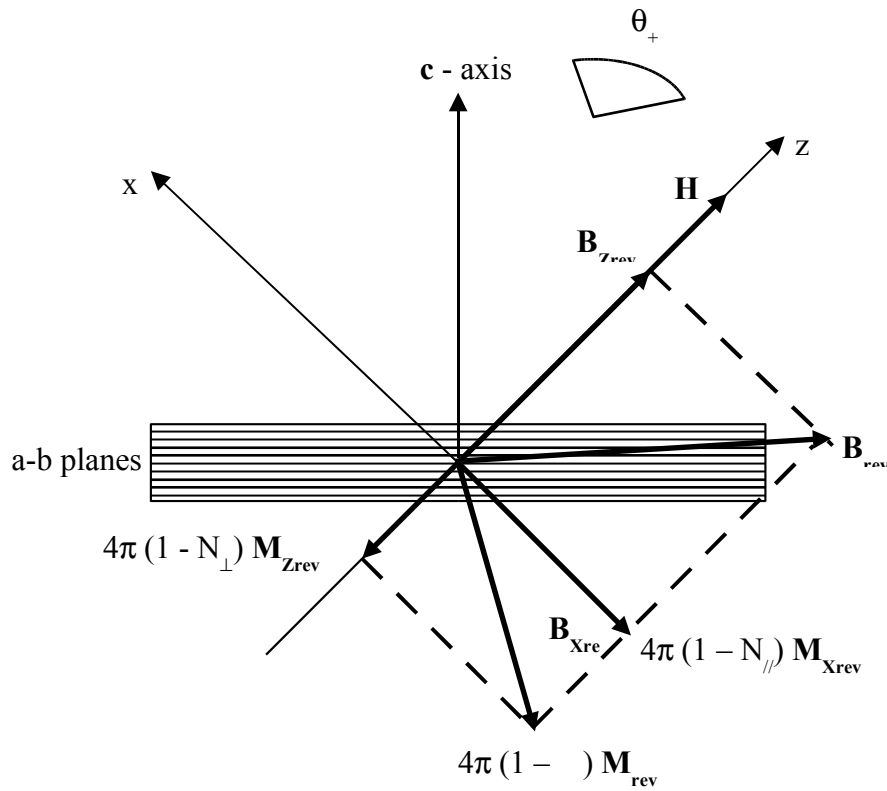
## RESULTS



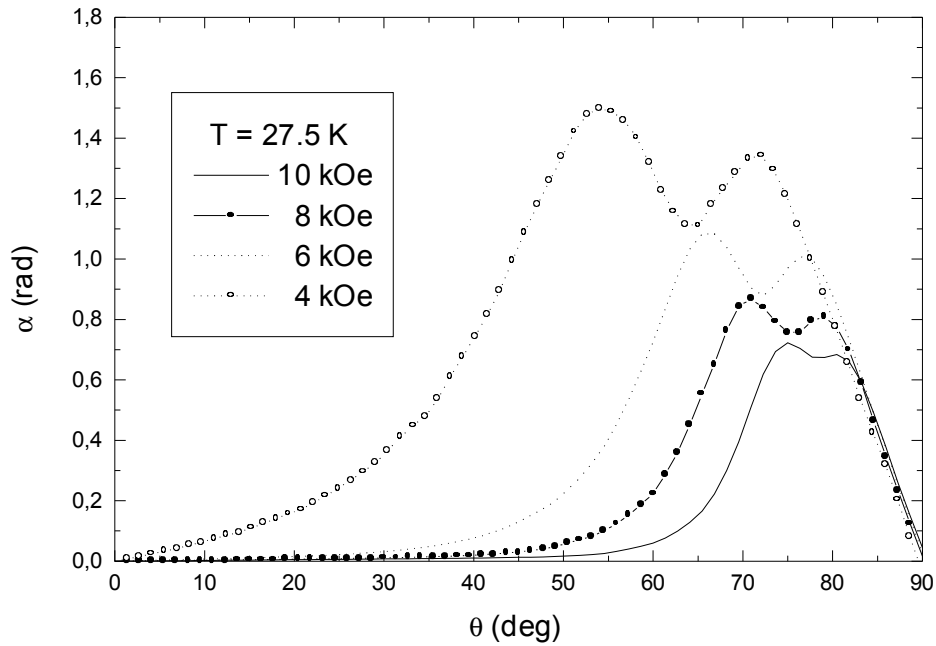
Scheme of double squid magnetometer with its orthogonal pick-up coils of Helmholtz type and representation of three degrees of liberty of the sample : a translatory motion  $T$  along of the  $z$ -axis, a rotational motion  $R_1$  round of the  $z$ -axis and a rotational motion  $R_2$  round the  $y$ -axis which permits to vary the angle  $\theta$  between the direction of applied magnetic field  $H$  and the  $c$ -axis of crystal (see Inset).



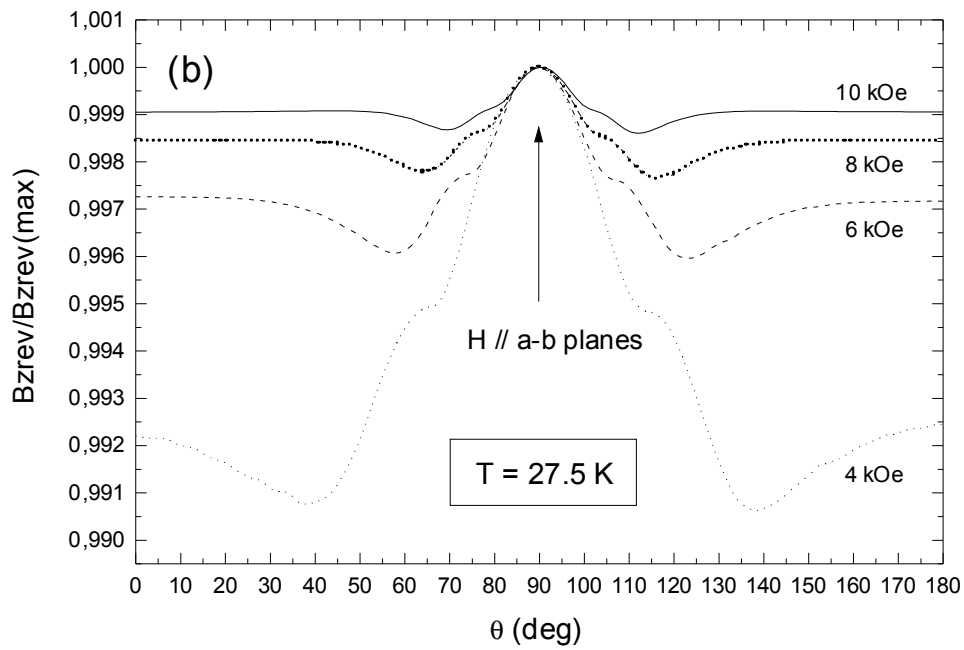
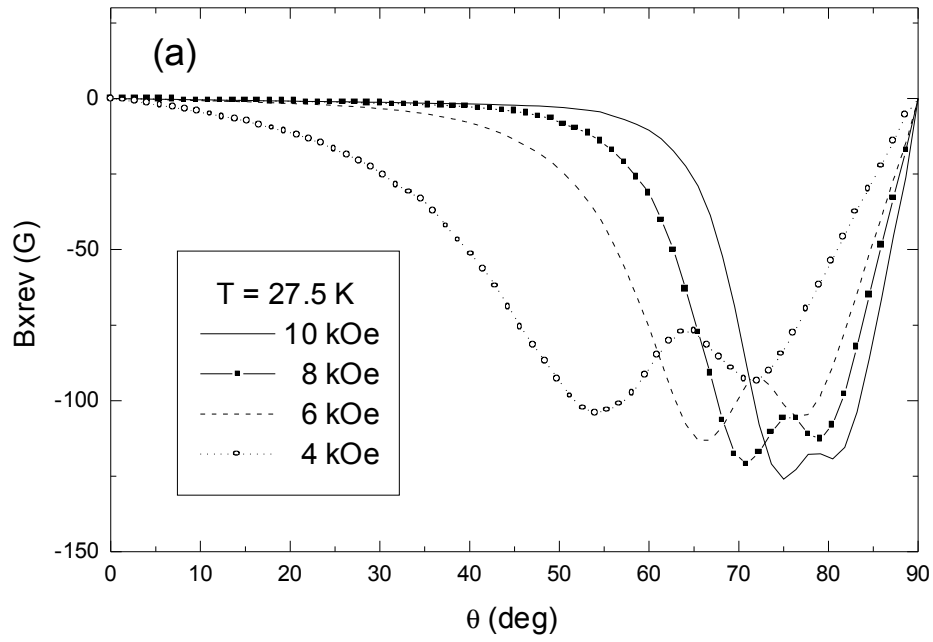
An example of variations of (a) transverse and (b) longitudinal magnetization components as a function of the orientation of crystal characterised by the angle  $\theta$  is shown at  $T = 27.5$  K and  $H = 4$  kOe. The reversal point indicates the place where the rotation angle is reversed.  $\theta_+$  and  $\theta_-$  symbolise forwarded and reversed rotation directions, respectively.



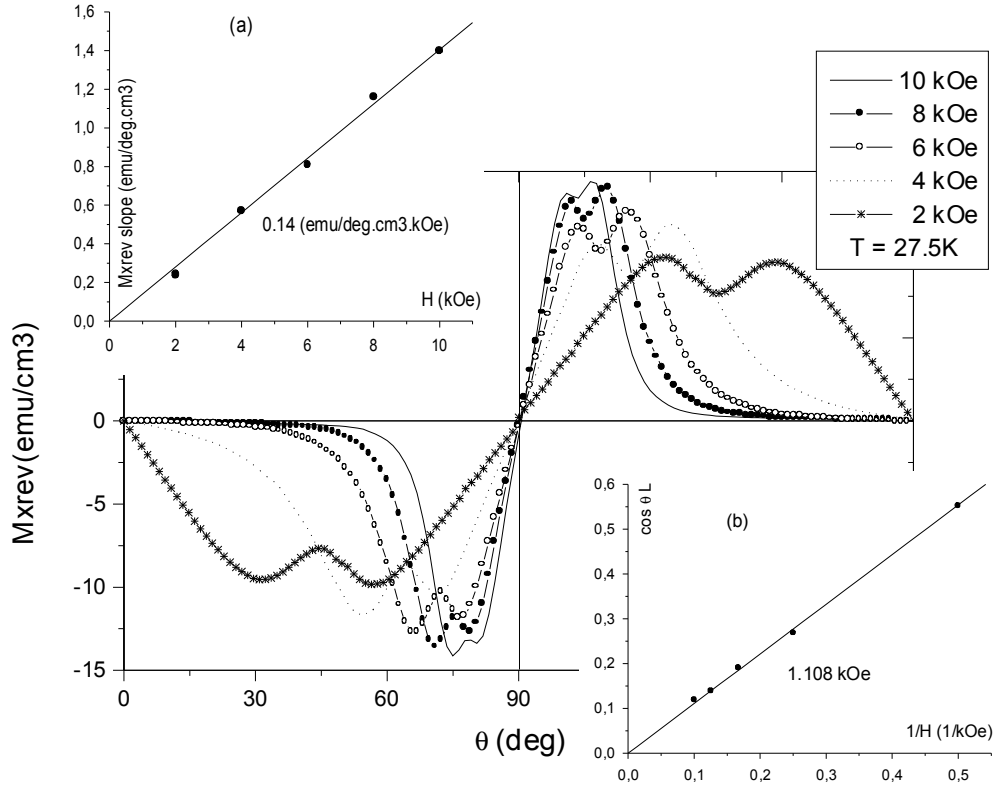
This vectorial construction shows the relation between the reversible magnetisation vector  $\mathbf{M}_{rev}$ , the reversible flux density vector  $\mathbf{B}_{rev}$  and the applied magnetic field  $\mathbf{H}$ . The symmetrical construction relative to the  $z$ -axis must be considered in the case where the rotation angle direction is reversed.



Variation of the angle  $\alpha$  between the reversible flux density vector  $\mathbf{B}_{\text{rev}}$  and the applied magnetic field vector  $\mathbf{H}$  as a function of the orientation of crystal characterised by the angle  $\theta$  for several values of applied field. We see that the angle  $\alpha$  increases again for a field applied closer to the plane than some critical angle field dependent (appearance of a second maximum near  $\theta = 90^\circ$ ).



Angular variations of (a) transverse ( $B_{Xrev}$ ) and (b) longitudinal ( $B_{Zrev}$ ) flux density components are shown at  $T = 27.5$  K and  $H = 4, 6, 8, 10$  kOe. In the locked state when the field is applied parallel to a-b planes, all the vortices sit between these planes and parallel to these later. As a result,  $B_{Xrev}$  must be rigorously null at  $\theta = 90^\circ$  (see Fig.a) and  $B_{Zrev}$  must reach its maximum value (see Fig.b).



Angular dependence of the reversible transverse magnetisation at  $T = 27.5$  K and  $H = 2, 4, 6, 8, 10$  kOe. The inset (a) shows the  $M_{Xrev}$  slopes close to  $\theta = 90^\circ$  for several values of applied field. Straight line is a fit to  $dM_{Xrev}/d\theta = A H$  with  $A = 0.14$  (emu.cm<sup>-3</sup>.deg<sup>-1</sup>.kOe<sup>-1</sup>). The variation of cosine of the lock-in angle  $\theta_L$ ,  $\cos(\theta_L)$ , as a function of the inverse of applied field ( $1/H$ ) is shown in the inset (b). We see that  $\cos(\theta_L)$  is proportional to  $1/H$  with a slope of  $1.108$  kOe.

### A NICE WAY TO LOOK FOR THE ANISOTROPY PARAMETER

In the 3-Dimensionnal Anisotropic Ginzburg-Landau Theory, the amount of the anisotropy is determined by the square root of effective mass of the quasi-particles flowing normal and parallel the CuO<sub>2</sub> planes  $\gamma = (m_{\perp}/m_{\parallel})^{1/2}$ . Within the London's limit ( $H_{C1} \ll H \ll H_{C2}$ ), the components of the magnetization are given by :

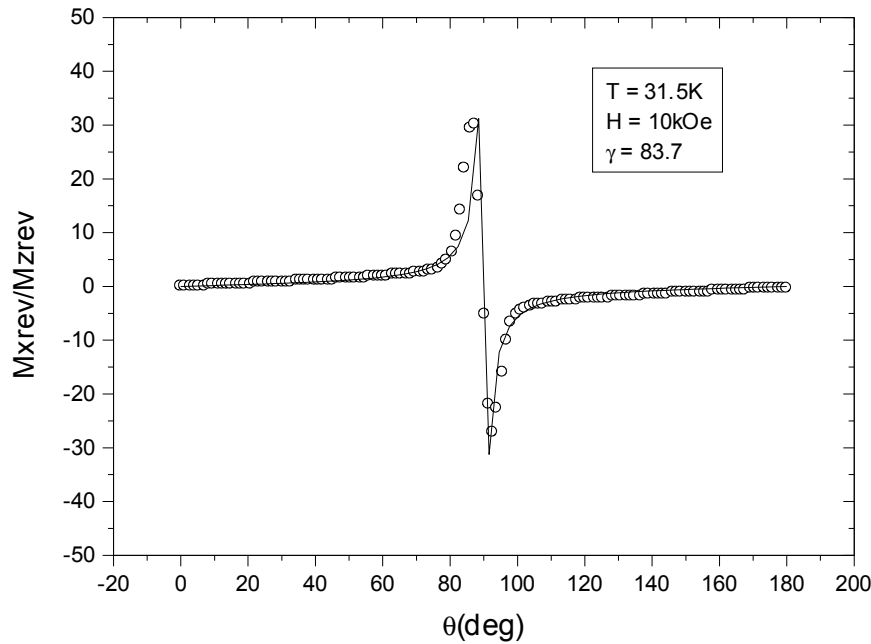
$$M_{X_{\text{rev}}} = - M_0 \frac{(\gamma^2 - 1) \sin(2\theta)}{2\varepsilon(\theta)} \ln \sqrt{\frac{\eta H_{C2//}(T)}{B}} \quad (1)$$

$$M_{Z_{\text{rev}}} = - M_0 \varepsilon(\theta) \ln \sqrt{\frac{\eta H_{C2//}(T)}{B}} \quad (2)$$

with  $\varepsilon(\theta) = \sqrt{\sin^2 \theta + \gamma^2 \cos^2 \theta}$  and  $M_0 = H_{C2//} / 8\pi\kappa_{//}^2$ .  $H_{C2//}$  is the upper critical field parallel to the planes and  $\kappa_{//}$  is the Ginzburg-Landau parameter for field applied parallel to the layers, it is equal to  $\kappa_{//} = \sqrt{\frac{\lambda_{//} \lambda_{\perp}}{\xi_{//} \xi_{\perp}}}$  where  $\lambda$  and  $\xi$  are the penetration depth and coherence length,

respectively.  $\eta$  is an undetermined parameter of the London approximation of the order of the unity. The ratio of those magnetization components (1) and (2) is expressed solely as a function of the anisotropy parameter  $\gamma$  (single fitting parameter):

$$\frac{M_{X_{\text{rev}}}}{M_{Z_{\text{rev}}}} = (\gamma^2 - 1) \frac{\sin \theta \cos \theta}{\sin^2 \theta + \gamma^2 \cos^2 \theta} \quad (3)$$



Angular variation of the ratio  $M_{Xrev}/M_{Zrev}$  of a  $\text{La}_{1.85}\text{Sr}_{0.15}\text{CuO}_4$  single crystal at  $T = 31.5 \text{ K}$  and  $H = 10 \text{ kOe}$ . The solid line is a fit to Eq.3 giving a value of the anisotropy parameter of 83.7.

## VORTICES PINNING EXTRINSIC

In conventional type II superconductors, impurities, defects, precipitates, and grains boundaries, work as pinning centers. The typical size of efficient inclusions is the coherence length, the diameter of the tube which is the normal state within the vortex. In high- $T_C$  oxide superconductors where the coherence length is very short ( $\xi \approx 10 \text{ \AA}$ ), it is obvious how to control the vortex pinning sites.

**AIM OF THIS STUDY : To discuss how the  $\text{Y}_2\text{BaCuO}_5$  (211 phase) precipitates affect the critical currents and the flux jumps.**

**Keywords : High- $T_C$  superconductors, Green phase inclusions (211 phase), Flux pinning, Critical current, Instability.**

• **Acknowledgements :**

I am very grateful to Louis Néel laboratory of Grenoble (France) for the use of large scientific facilities, to Pr. B. Barbara for his financial support and to Pr. H. Noël of Rennes University (France) for the preparation of the samples

**MAIN IDEAS OF THE DYNAMIC DESCRIPTION BASED UPON  
THE THEORY OF COLLECTIVE PINNING**

(L. Krusin-Elbaum et al. Physical Review letters, Vol 69, N°15 (1992) 2280)

• **Single-vortex (1D) pinning regime** : In a static picture (i.e. without creep) the relevant length in 1D regime is  $L_C$ , the longitudinal correlation length. If  $L_C$  is less than the intervortex spacing  $a_0 = (\Phi_0/B)^{1/2}$  the vortices are pinned independently and  $J_C$  is determined by pinning barriers for single vortices.

• **Collective (3D) pinning regime** : At high enough temperatures or fields, the intervortex interaction becomes significant. The two relevant lengths are now  $L_C$  and  $R_C > a_0$ , the longitudinal and transverse size of correlated region, respectively. In this regime the critical current  $J_C$  is controlled by collective pinning of vortex bundles confined by a correlation volume and is field dependent.

• **Various regimes of collective pinning** :

- At low fields the observed current  $J$  is dominated by collective creep, at high fields (the large bundles regime) the pinning energy is larger hence the relaxation is small and the field dependence of  $J$  is essentially determined by  $J_c$  ( $H$ ).
- A transition from nonlocal regime ( $R_c \leq \lambda$ ) to local regime ( $R_c > \lambda$ ).
- The irreversibility line which is assumed to separate a pinned vortex solid from unpinned vortex liquid.

## EXPERIMENTAL PROCEDURE

☞ Three Y-Ba-Cu-O single crystals used

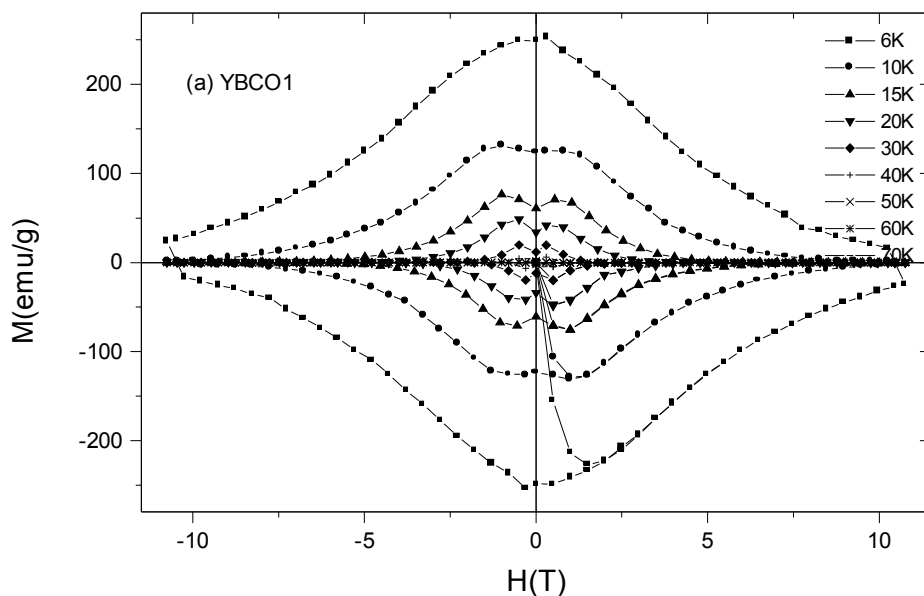
- ☉ YBCO1 :
  - $T_c = 65.5$  K
  - dimensions :  $3.66 \times 3.44 \times 0.49$  mm<sup>3</sup>
  - mass =  $34.0 \pm 0.1$  mg
- ☉ YBCO2 :
  - $T_c = 92$  K
  - dimensions :  $1.6 \times 1.32 \times 0.49$  mm<sup>3</sup>
  - mass =  $6.7 \pm 0.1$  mg
- ☉ YBCO3 :
  - $T_c = 86$  K
  - dimensions :  $0.8 \times 0.8 \times 0.2$  mm<sup>3</sup>
  - mass =  $2.8 \pm 0.1$  mg

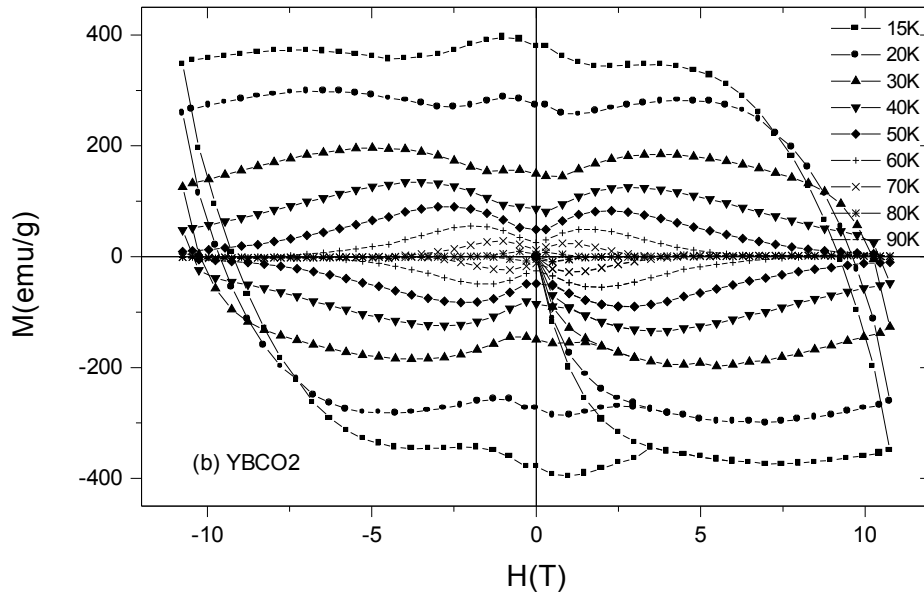
☉ originate in the same batch

☉ prepared by melt-growth method

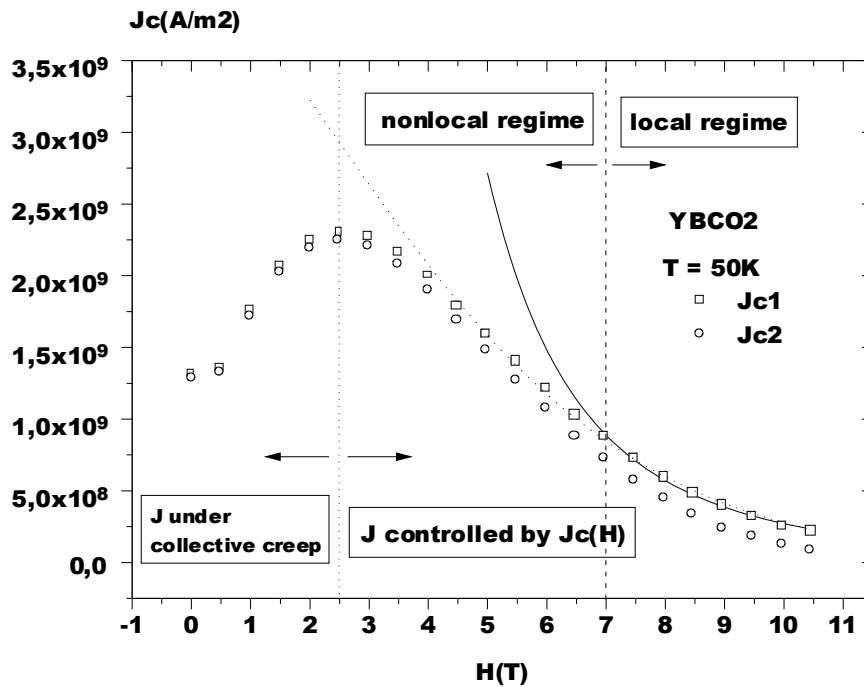
- two crystals contain the 211 phases, in different proportions; the reference third sample devoid of these phases
- prepared by H. Noël (Rennes University, France)
- Neutron diffraction experiments showed these blocks were single crystals but because of their growth temperature, close to peritectic decomposition, the presence of some green phase inclusions in the largest blocks was unavoidable.
- ☞ Magnetization loops measured using a conventional magnetometer
  - in an applied magnetic-field range between  $-11$  and  $11$  T
  - for several temperatures and field sweep rates
  - For a field applied parallel and perpendicular to  $c$ -axis of the sample
- ☞ Samples heated above the transition temperature between two measurements
- ☞ Field reversed to obtain the total hysteresis loop

## RESULTS

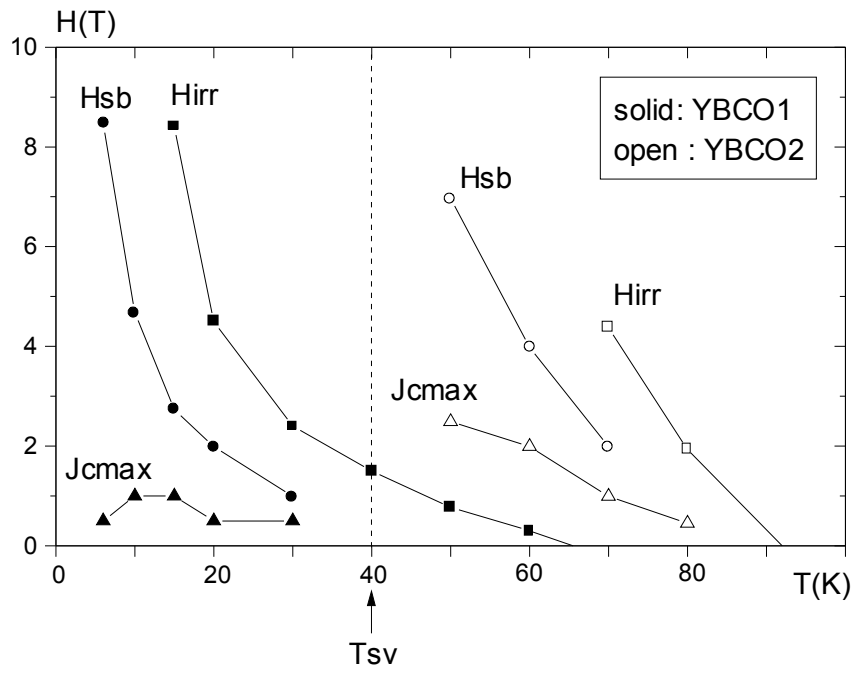




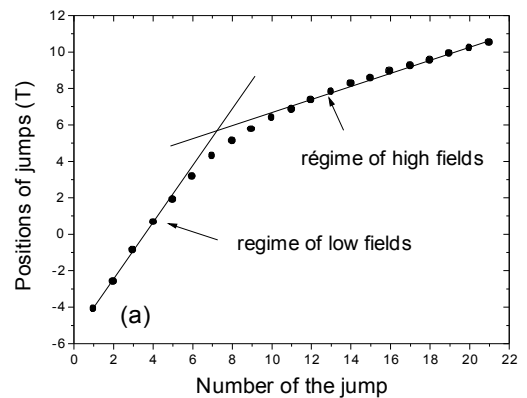
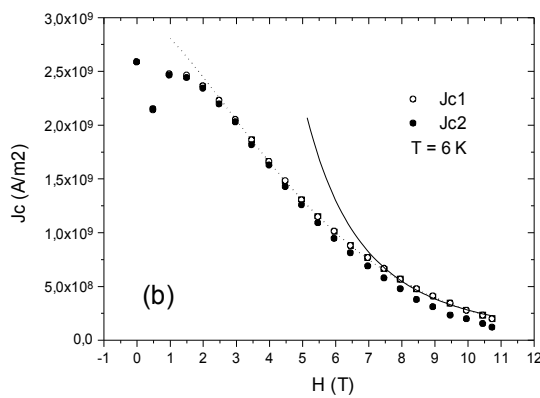
Magnetization curves  $M(H)$  obtained in both crystals for several temperatures and for an applied field parallel to the  $c$ -axis.

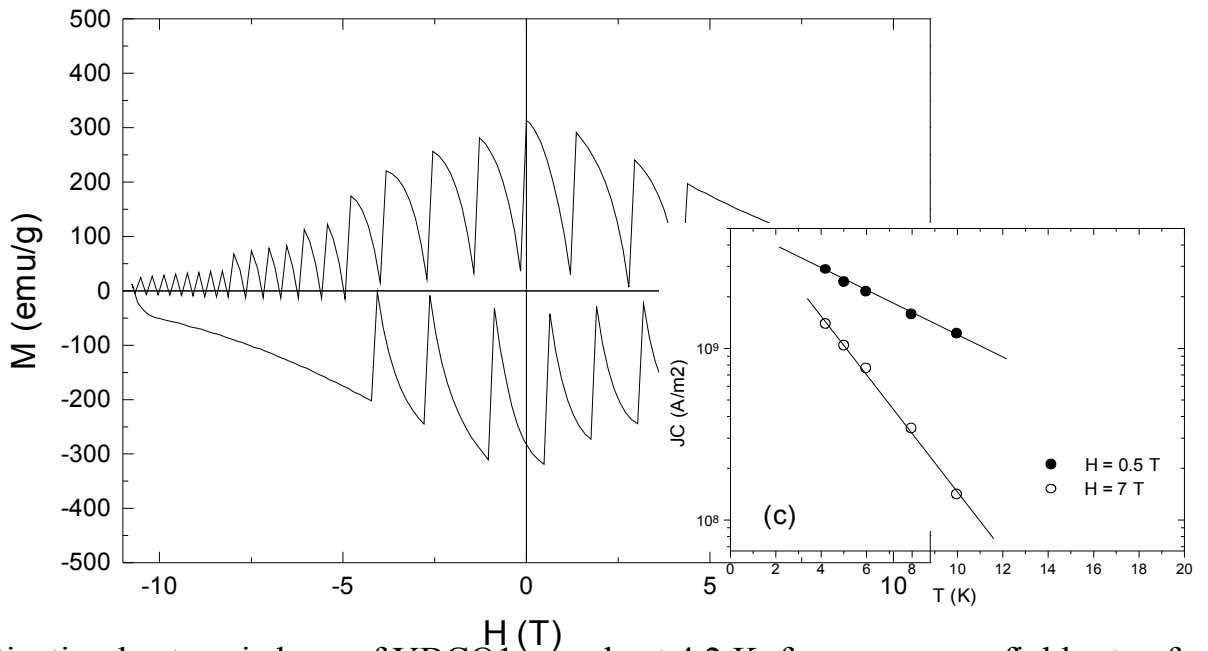


Field variation of  $J_{c1}$  and  $J_{c2}$  of YBCO<sub>2</sub> corresponding to the first and the second measurement, respectively at 50K (in the 3D regime). Note that  $J_{c1}$  and  $J_{c2}$  are joined up to the maximum of  $J_c(H)$ . Full line is a fit to  $J_c = A/H$  for  $H \geq 6.97$  T with  $A = 3.12 \times 10^{11}$  T<sup>3</sup> A/m<sup>2</sup>. Dotted line is a fit to  $J_c = \alpha \exp(-\beta H^{3/2})$  with  $\alpha = 4.1 \times 10^9$  A/m<sup>2</sup> and  $\beta = 0.085$  T<sup>-3/2</sup>,  $\beta$  contains the temperature dependence of  $H_{c2}$ , the pinning strength.

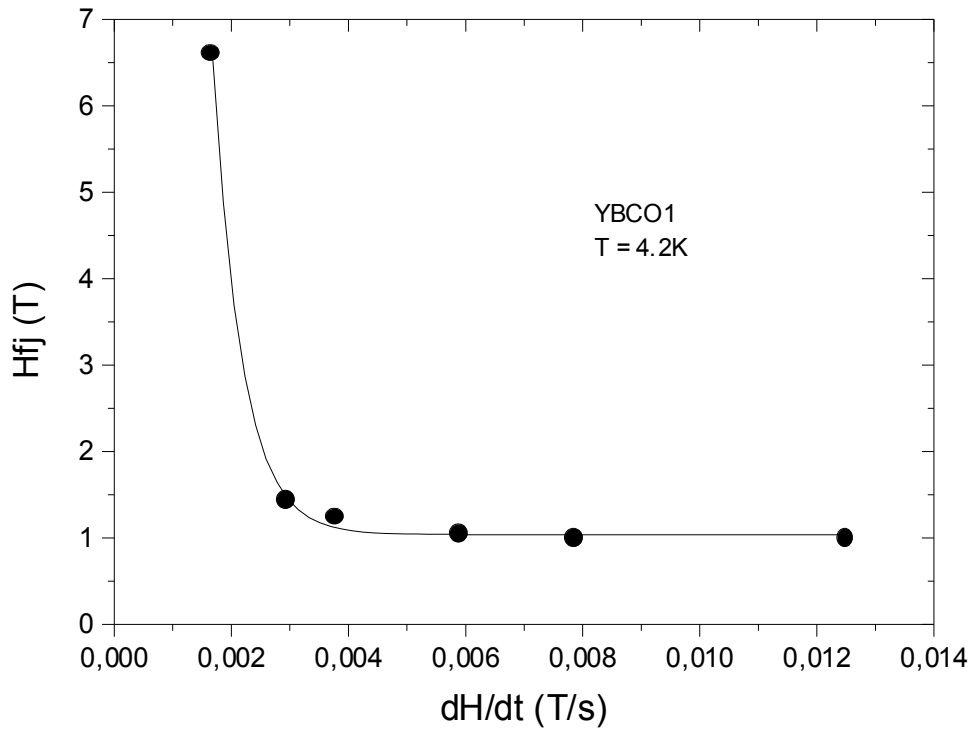


Phase diagram showing for each crystal the collective pinning boundaries; all the solid lines are a guide to eye. The vertical dashed line at  $T = T_{sv}$  denotes a transition from the single vortex to collective pinning regime. In the YBCO2 case, this transition occurs nearly at 40 K. In the YBCO1 case, for all studied temperatures this crystal is found to be in the collective pinning regime. The circles indicate a crossover from nonlocal to local regime. The up triangles are a guide to eye through the maximums of  $J_c$ ; they separate the region controlled by relaxation and one controlled by  $J_c(H)$ . The squares represent the irreversibility line. The collective pinning boundaries of YBCO1 are displaced towards lower field and temperature because of low pinning in this crystal.





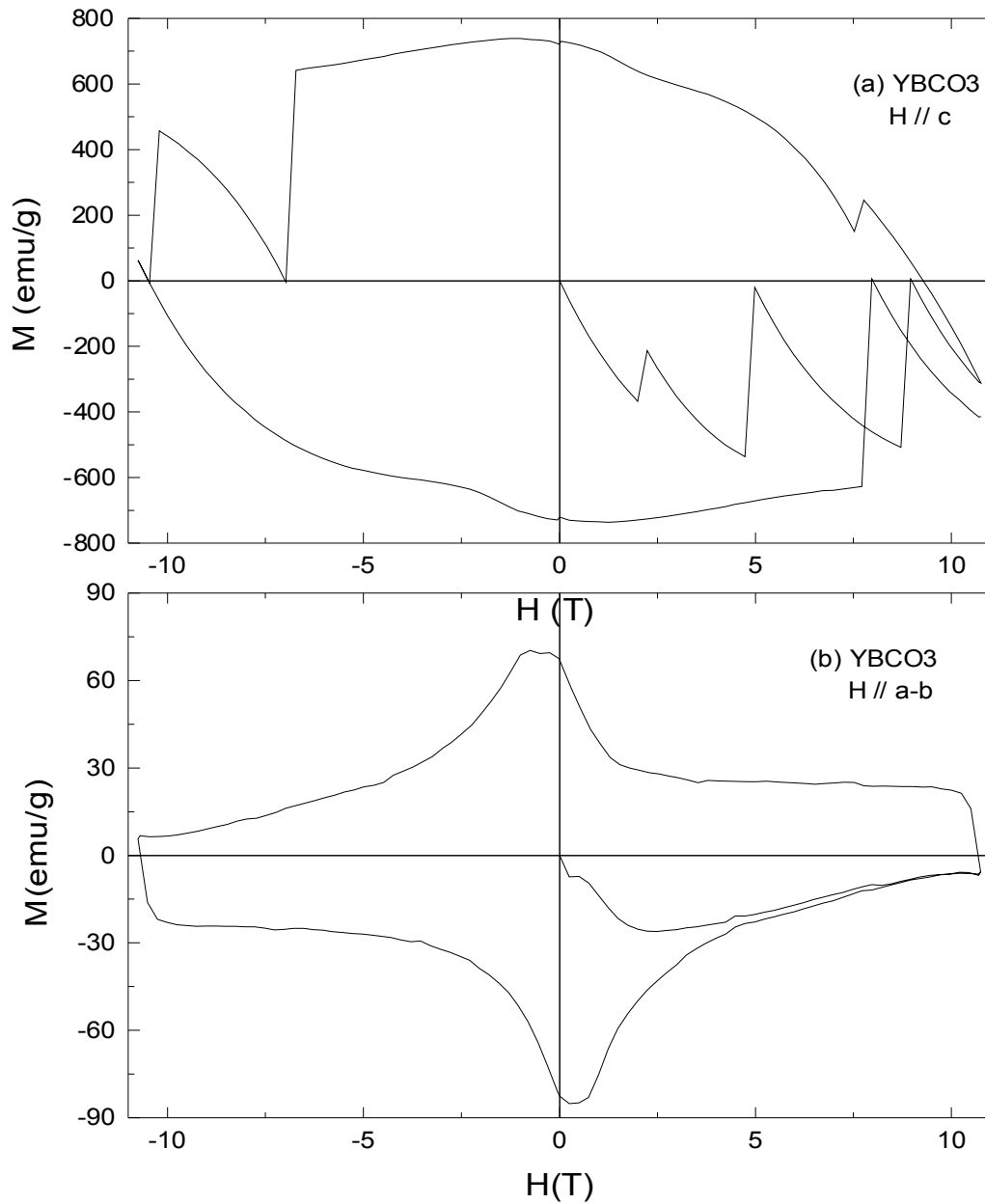
Magnetization hysteresis loop of YBCO1 sample at 4.2 K, for an average field rate of 0.00295 T/s. Note that the spacing of flux jumps is more important in the low fields region than in that of high fields. (Inset a) : Positions of flux jumps versus number of the jump derived from the hysteresis cycle of Fig.1. A crossover is observed between the region of low fields and that of high fields. Solid lines are a guide to the eye. (Inset b) : Field variation of the critical current densities  $J_{C1}$  and  $J_{C2}$  of YBCO1 sample corresponding to the first and the second measurement, respectively, at 6 K. Note that  $J_{C1}$  and  $J_{C2}$  are joined up to the maximum of  $J_c(H)$ . Full line is a fit to  $J_c = A/H^3$  for  $H \geq 7.47$  T with  $A = 2.81 \times 10^{11}$  T<sup>3</sup>A/m<sup>2</sup>. Dotted line is a fit to  $J_c = \alpha \exp(-\beta H^{3/2})$  with  $\alpha = 3.03 \times 10^9$  A/m<sup>2</sup> and  $\beta = 0.075$  T<sup>-2/3</sup>. (Inset c) : Temperature dependence of critical currents of YBCO1 at low temperatures ( $T \leq 10$  K), derived from the hysteresis loops for  $H // c$  and two values of the applied field. Solid lines are a guide to the eye showing that for a given value of applied field there is no physical difference in temperature dependence of  $J_c(T)$  (no change of slope).



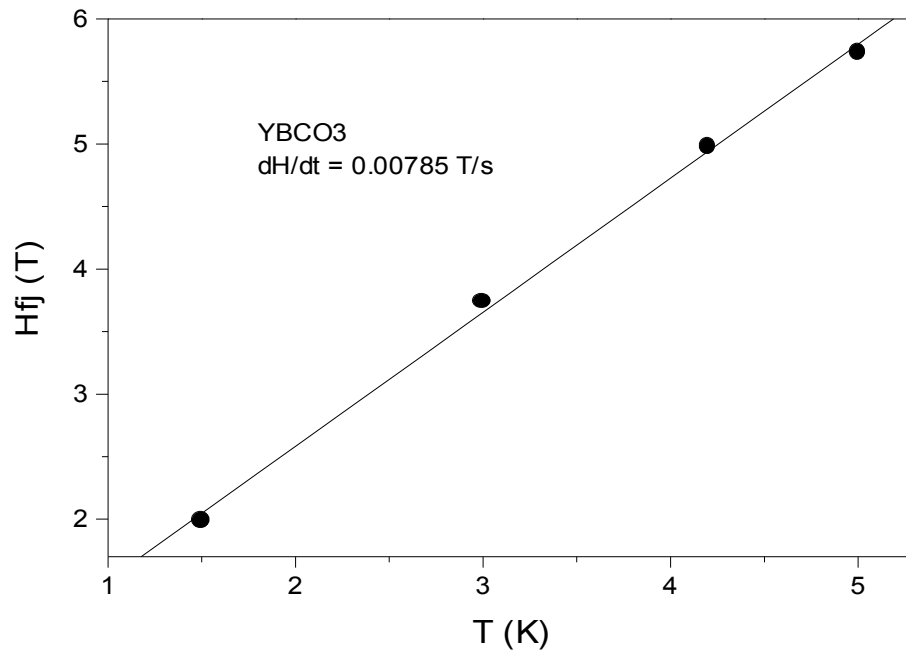
Data of jump-starting field  $H_{fj}$  versus field rate at  $T = 4.2$  K, for YBCO1 sample. Full line is a fit of Eq.:

$$H_{fj} = a + b \exp\left(\frac{dH/dt}{c}\right)$$

with  $a = 1.04$  T,  $b = 164.8$  T and  $c = 0.0005$  s/T.



The magnetization of YBCO<sub>3</sub> sample is shown at 1.5 K and  $dH/dt = 0.00785$  T/s, for two field orientations. (a) H // c. (b) H  $\perp$  c. Note the absence of flux jumps for this particular direction of the applied field indicating that the 211 phase inclusions constitute a factor of stabilisation for YBCO, at least for this particular direction of the applied field.



Data of the first jump field  $H_{fj}$  at a average field rate of 0.00785 T/s and  $T = 1.5, 3, 4.2$  and 5 K. Straight line is a fit to of Eq.:

$$H_{fj} = a + b T$$

with  $a = 0.44$  T and  $b = 1.07$  T/K. We see that the jump-stating field  $H_{fj}$  is linearly proportional to the temperature T.